Available online at www.sciencedirect.com

ScienceDirect

Energy Procedia 122 (2017) 649–654

Energy Procedia

www.elsevier.com/locate/procedia

CISBAT 2017 International Conference Future Buildings & Districts Energy Efficiency from Nano to Urban Scale, CISBAT 2017 6-8 September 2017, Lausanne, Switzerland

Daylighting & Electric Lighting (Green Lighting)

Characterization of a quasi-real-time lighting computing system based on HDR imaging

Yujie Wu[a], Jérôme Henri Kämpf[b], Jean-Louis Scartezzini[a]

[a] *Solar Energy and Building Physics Laboratory (LESO-PB), École polytechnique fédérale de Lausanne (EPFL), CH-1015, Lausanne, Switzerland*
[b] *Haute école d'ingénierie et d'architecture Fribourg (HEIA-FR), CH-1705, Fribourg, Switzerland*

Abstract

In this paper we present the characterization of a calibrated embedded system for quasi real-time lighting computation based on HDR sky monitoring. To quantify its accuracy in lighting computation, we positioned the device in front of a test module with unilateral-façades to measure the luminance distribution of the sky and ground dome, including that of the sun, the clouds and landscape, followed by on-board illuminance computation in the device. An experiment was conducted on two representative days, with overcast and clear sky respectively. The embedded device computed the illuminance for 5 virtual sensors which was referred to the measurement by 5 lux-meters at the identical positions synchronously to assess its relative error. Compared with the Perez all-weather sky model, the embedded device was indicated to be more reliable and achieved 10%-25% higher accuracy in transient lighting computation of horizontal illuminance based on HDR imaging and luminance mapping.

Peer-review under responsibility of the scientific committee of the CISBAT 2017 International Conference – Future Buildings & Districts – Energy Efficiency from Nano to Urban Scale

Keywords: Real-time; Lighting simulation; Embedded system; FPGA; Horizontal illuminance

1. Introduction

Daylight offers buildings and occupants a cost-effective source of illuminant, however, excessive or scarce daylight impacts negatively on the energy savings of artificial light [1], health of occupants [2] and productivity of office users [3]. The simulation of daylight in many ways acts as a reference of performance analysis in buildings, providing the possibility for designers to pre-plan the smart utilization of daylight. With the recent proliferation of user centric research [4,5], lighting simulation further unveiled its merit in visual comfort assessment [6]. In addition, the trend of architecture design, covering the building with a large area of glazing, imposes further demands on the regulation

* Yujie Wu. Tel.: +41-21-693-3435 ; fax: +41-21-693-2722.
E-mail address: yujie.wu@epfl.ch

1876-6102
Peer-review under responsibility of the scientific committee of the CISBAT 2017 International Conference – Future Buildings & Districts – Energy Efficiency from Nano to Urban Scale
10.1016/j.egypro.2017.07.364

of daylight due to its increased penetration. Against this background, the formulation of optimal daylight control will require further accuracy of transient lighting simulation.

The fidelity of lighting computation is fundamentally limited by a number of factors including the mismatch of material property and geometry between the modelled and real scene, the employed sky models and computational algorithms. A recent study indicated that sky models had a pronounced influence on the results of lighting simulation [7]. The uniform sky model is phasing out for transient simulation, as its presumption of a oversimplified homogeneous sky contributes to substantial errors. The standard CIE sky assumes a generic sky model according to the geometric location, date, time and 15 different pre-defined sky types [8]. The limitation of the model is that it is not dynamic according to the mutation of the real sky. The commonly used Perez all-weather sky model is relatively more advanced and dynamic, based on direct normal and diffuse horizontal irradiance to predict the sky conditions. Although it is more reliable for transient analysis, the nature of sub-sampling with only two input filters out high spatial-frequency components of the sky such as complex patterns of the clouds and high contrast patches of the sky. HDR (High dynamic range) imaging based lighting simulation was indicated with superiority over the simple sky models with a large number of pixels as input [9]. If its imaging system can be comprehensively calibrated, the accuracy of the HDR imaging based approach can be improved and be potentially compared to reliable reference.

This paper investigates the accuracy of a calibrated embedded device [10] in horizontal illuminance computing, which integrates both the quasi real-time HDR monitoring of the sky and on-board lighting simulation. The dynamic range of luminance that the device can measure ranges from 10^2 to 3.1×10^9 cd/m^2 (150 dB), covering that of both extremes of the direct sun and the surrounding landscape during daytime. The resolution of the device can map the sky and ground dome up to 1.25×10^6 patches, including the sun, the sky, clouds and surrounding landscape. The high resolution mapping, at the same time, saves the effort to model the landscape, especially for vegetation including trees which are formidably difficult to model. As the device can potentially be applied in photo-realistic rendering, evaluation of lighting performance parameters and building automation, the accuracy of the device to simulate transient lighting performance parameters characterizes its reliability and applicability. In this paper, we try to formulate an intra-scene experiment to investigate the relative error of the device in horizontal illuminance computation in comparison with the commonly used Perez all-weather model in a simplified test module.

2. Methodology

The embedded device is mainly composed of a field programmable gate array (FPGA) chip, DDR3 memory and an image sensor. The FPGA, as a fast speed micro-controller, controls the image sensor to capture images of the sky dome, synthesises them into a luminance map and computes lighting in a quasi real-time manner. The image sensor is coupled with a wide angle lens to enable its field of view (FOV), subtending the majority area of the sky and ground hemisphere and, at the same time, keep the distortion at a reasonable level. The spectral response of the image sensor was calibrated according to the luminosity function reaching f'1 error at 8.86% by color filters together with neutral density filters. Its vignette and geometric distortion were also rectified digitally.

For the lighting computation algorithm, the RADIANCE program was employed in this paper, which was largely developed by Greg Ward in LBNL, EPFL and SGI [11]. RADIANCE is a physically-based lighting program package utilizing backward ray-tracing algorithms, which is open source and has been widely used in the lighting simulation by researchers due to its reliability. The lighting computation, in this paper, focused on the rtrace sub-program based on Monte-Carlo integration for the glow material, with high quality parameters.

A recently retrofitted test module (interior size: $6.4 \times 2.9 \times 2.6\, m^3$) was selected as the target scene for experiments due to its simplified set-up. The test module was coupled with 6 unilateral façades reaching 0.62 window-to-wall ratio, which were facing towards south. The module was equipped with 3 desks resembling a typical office. To establish the model in RADIANCE, the geometric size and relative position of furnitures in the module were measured by a range finder (Leica DISTO). The color, specularity and roughness property of the each surface were determined to model the reflection of the scene in RADIANCE, including the ceiling, the wall, the floor, the window frame and each surface of furnitures. We employed a chromameter (MINOLTA CR-220) to measure the color and reflectance of each material in xyY color space with D65 light source. The xyY color coordinates were further transformed to the RGB color space respectively according the color primaries defined in RADIANCE. The specularity of the material was measured and approximated by a gloss meter (MINOLTA GM-060), which characterized the percentage of the specular component of reflected light at 60° incident angle. Although in reality this ratio might alter according to the incident angle, in this paper, it was approximately regarded to be constant. In addition, the roughness was set at 0 ∼ 0.2 according to the particle size of each surface. Finally the scene was modelled in RADIANCE.

In order to monitor the horizontal illuminance as a reference, 5 lux-meter sensors (MINOLTA T-10A) were positioned in the test module at 0.8 m height above the floor as work-plane, with distance of 1 m, 2 m, 3 m, 3.9 m and 4.7 m to the façade, as illustrated in Fig. 1. Each lux-meter was connected to a data logger in parallel in a way the output of each sensor can be recorded simultaneously. Accordingly, 5 virtual illuminance sensors were defined in RADIANCE at the identical positions as the scene respectively to simulate the illuminance for each. As the virtual sensors are point sensors in RADIANCE, 9 points in a $2\times2\ cm^2$ square were computed and averaged to represent each virtual sensor, which, at the same time, mitigated spatial random noise. The computed illuminance is to be compared with the measured value by lux-meters as reference to calculate the relative error.

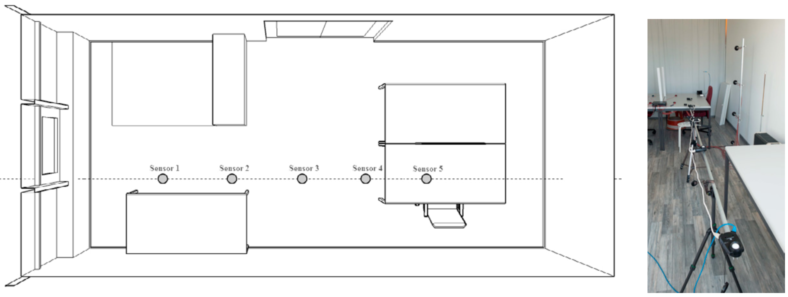

Fig. 1: Position of lux-meter sensors

3. Experiments and Results

After the scene was established in the embedded device, we anchored the device in front of the test module with the axis of lens in the orthogonal plane to the façade, subtending the hemisphere of sky and ground dome that the façade was facing towards, as displayed in Fig. 2. The luminance map of the sun, the sky and landscape was monitored and generated by the embedded device and synthesised into the scene in RADIANCE. The micro-processor then implemented the on-board illuminance computation based on Monte-Carlo integration in RADIANCE.

Fig. 2: Embedded device positioned in front of the test module

The real-site experiment was conducted on one day with clear sky and another day with overcast sky as two extreme conditions for the evaluation of the accuracy of the device. The device monitored the sky, generated the luminance map and accomplished the illuminance computing for the 5 virtual sensors every 15 minutes from 9 a.m. to 6 p.m. for the test module. Accordingly, the 5 real lux-meter sensors were synchronized with the embedded device to record the measured illuminance every 15 minutes. At the same time, the direct normal and diffuse horizontal irradiance were monitored at the rooftop of the laboratory. For comparison of performance, the irradiance data was used for the illuminance simulation by employing the Perez all-weather model for the identical virtual sensors in the test module with the same sets of parameters.

Fig. 3 (a) displays the results of the transient illuminance, under a predominant overcast sky, recorded by the lux-meter (gray dotted line) and that computed by the embedded device (green solid line) based on HDR imaging respectively, which stacked from top to bottom sequentially for Sensor 1 (close to the façade) to Sensor 5 (far from the façade). In contrast, the computed illuminance based on the Perez all-weather sky model was presented in a similar way in Fig. 3 (b). According to the results, illuminance computed by the embedded device shows closer proximity and better accordance to the reference than using the Perez sky model, which can be further illustrated by their transient relative error in Fig. 4 (a) and (b) respectively. The average relative error of the 5 virutal sensors throughout a day was 6.4%, 7.5%, 4.1%, 5.0% and 7.0% respectively computed by the embedded device based on HDR imaging relative to the lux-meters as reference, while that of the Perez all-weather model was 32%, 22%, 29%, 23% and 23% respectively. The overall higher error rate of the Perez sky model for a overcast day can possibly be attributed to the neglected complex cloud patterns and commonly non-smooth distribution of the luminance of the sky and ground dome.

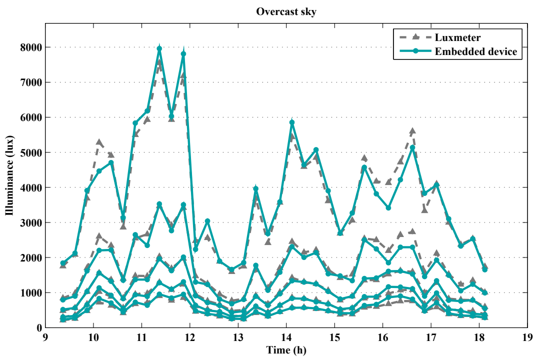

(a) HDR imaging

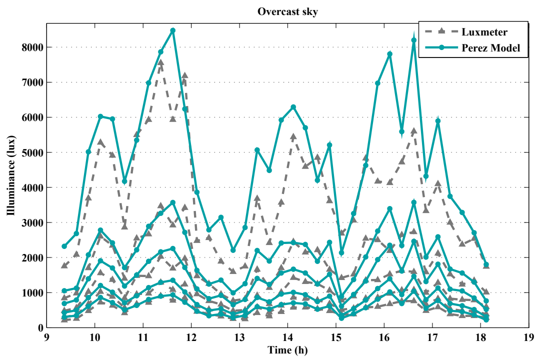

(b) Perez all-weather sky model

Fig. 3: Measured and computed illuminance for a day with overcast sky

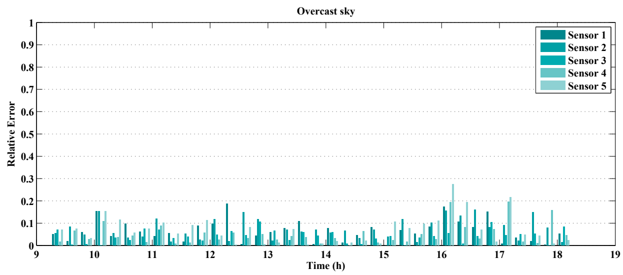

(a) HDR imaging

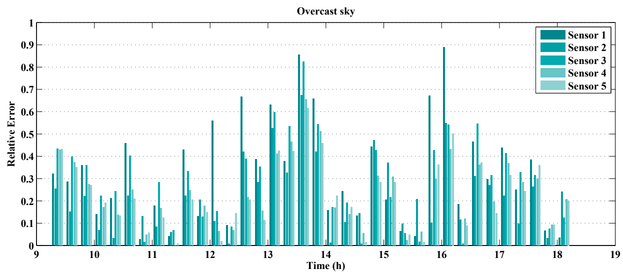

(b) Perez all-weather sky model

Fig. 4: Relative error of computed illuminance for a day with overcast sky

For a day with predominant clear sky, Fig. 5 (a) in the same way illustrates the transient illuminance recorded by the lux-meter (gray dotted line) and that computed by the embedded device (green solid line). For comparison, the illuminance computed by employing the Perez all-weather sky model was presented in Fig. 5 (b). Although illuminance computed by the embedded device again emulated closer to the reference than the Perez sky model as illustrated in Fig. 6 for the transient relative error, sensors close to the façades (Sensor 1 and Sensor 2) had a relatively noticeable error from 9:30 to 11:30 a.m.. This might originate from the fact that, in the luminance map of the sky, the sun was not extracted from the sky background and not separately defined in RADIANCE, which possibly resulted in insufficient sampling and thus the underestimated the contribution of lighting from the direct sun disk. The average relative error of the 5 virutal sensors computed by the embedded device based on HDR imaging compared with the lux-meters as reference was 25%, 22%, 9.7%,, 8.9% and 11% respectively, while that of the Perez all-weather model was 37%, 32%, 36%, 31% and 28%.

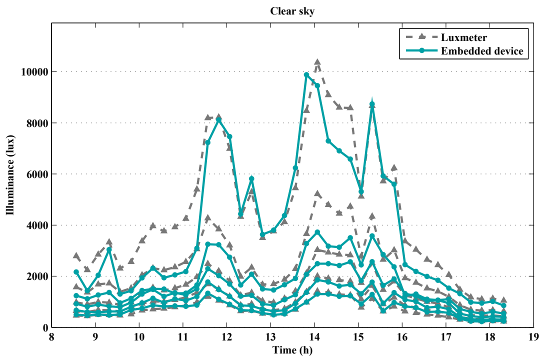

(a) HDR imaging

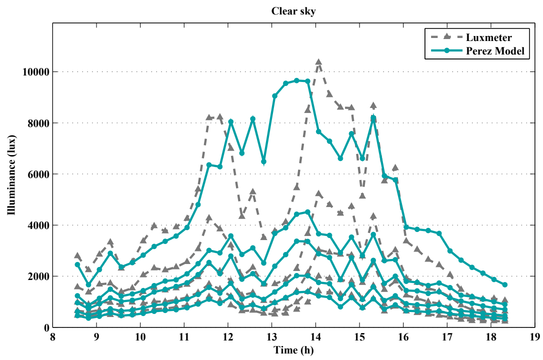

(b) Perez all-weather sky model

Fig. 5: Measured and computed illuminance for a day with clear sky

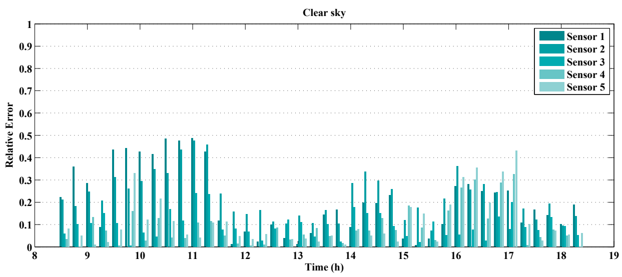

(a) HDR imaging

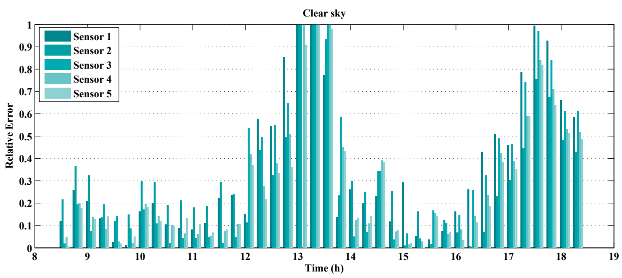

(b) Perez all-weather sky model

Fig. 6: Relative error of computed illuminance for a day with clear sky

4. Conclusion

In this paper, a calibrated embedded system integrating the HDR sky monitoring and on-board lighting simulation was evaluated in its accuracy in computing the horizontal illuminance distribution for intra-scene application in a test module compared with employing Perez all-weather sky model. Although both showed proximity as referred to measurement by lux-meters, the embedded system was expected with 15%-25% less error in horizontal illuminance computation for an overcast sky compared with that employing the Perez all-weather sky model based on direct normal and diffuse horizontal irradiance. In the case of a clear sky, the error of the device was expected to be 10%-20% less than employing the Perez all-weather sky model. During the experiments, it was found that the error during the exposure to the direct sun disk contributed to noticeable error in computing the illuminance at positions close to the façade, which might be the result of non-sufficient sampling in the Monte-Carlo integration under conditions of extreme contrast in luminance map. This can possibly be improved by extraction of the solar component from the luminance map and concentrated sampling of the sun disk by RADIANCE, which will be explored in our future work.

Acknowledgements

The authors would like to thank the Commission for Technology and Innovation of Switzerland for funding Swiss Competence Center for Energy Research (SCCER), Future Energy Efficiency Buildings and District (FEEB&D).

References

[1] F. Linhart and J.-L. Scartezzini, “Evening office lighting visual comfort vs. energy efficiency vs. performance?,” *Building and Environment*, vol. 46, no. 5, pp. 981 – 989, 2011.

[2] R. Kller, S. Ballal, T. Laike, B. Mikellides, and G. Tonello, “The impact of light and colour on psychological mood: a cross-cultural study of indoor work environments,” *Ergonomics*, vol. 49, no. 14, pp. 1496–1507, 2006. PMID: 17050390.

[3] T. Chung and J. Burnett, “Lighting quality surveys in office premises,” *Indoor and Built Environment*, vol. 9, no. 6, pp. 335–341, 2000.

[4] P. Iacomussi, M. Radis, G. Rossi, and L. Rossi, “Visual comfort with {LED} lighting,” *Energy Procedia*, vol. 78, pp. 729 – 734, 2015. 6th International Building Physics Conference, {IBPC} 2015.

[5] M. Frascarolo, S. Martorelli, and V. Vitale, “An innovative lighting system for residential application that optimizes visual comfort and conserves energy for different user needs,” *Energy and Buildings*, vol. 83, pp. 217 – 224, 2014. {SCIENCE} {BEHIND} {AND} {BEYOND} {THE} {SOLAR} {DECATHLON} {EUROPE} 2012.

[6] L. Fernandes, E. Lee, and G. Ward, “Lighting energy savings potential of split-pane electrochromic windows controlled for daylighting with visual comfort,” *Energy and Buildings*, vol. 61, pp. 8 – 20, 2013.

[7] M. Inanici and A. Hashemloo, “An investigation of the daylighting simulation techniques and sky modeling practices for occupant centric evaluations,” *Building and Environment*, vol. 113, pp. 220 – 231, 2017. Advances in daylighting and visual comfort research.

[8] ISO 15469:2004(E) / CIE S 011/E:2003, “Spatial distribution of daylight - CIE standard general sky,” Standard, Commision Internationale de l’Eclairage, Vienna, Austria, 2003.

[9] M. Inanici, “Evalution of high dynamic range image-based sky models in lighting simulation,” *LEUKOS*, vol. 7, no. 2, pp. 69–84, 2010.

[10] Y. Wu, J. H. Kämpf, and J.-L. Scartezzini, “An embedded system for quasi real-time lighting computation based on sky monitoring,” in *Building Simulation*, (San Francisco, California), IBPSA, Aug 2017.

[11] G. W. Larson, R. Shakespeare, and C. Ehrlich, *Rendering with radiance : the art and science of lighting visualization*. The Morgan Kaufmann series in computer graphics and geometric modeling, San Francisco, California: Morgan Kaufmann, 1998.